Three-dimensional metamaterial nanotips

S. Mühlig,[1] C. Rockstuhl,[1] J. Pniewski,[2] C. R. Simovski,[3] S. A. Tretyakov,[3] and F. Lederer[1]
[1]*Institute of Condensed Matter Theory and Solid State Optics, Friedrich-Schiller-Universität Jena, Max-Wien-Platz 1, 07743 Jena, Germany*
[2]*Faculty of Physics, University of Warsaw, Pasteura 7, 02-093 Warsaw, Poland*
[3]*Department of Radio Science and Engineering/SMARAD, Helsinki University of Technology, P.O. Box 3000, FI-02015 TKK Espoo, Finland*

(Received 9 November 2009; revised manuscript received 28 January 2010; published 22 February 2010)

We investigate the optical properties of a three-dimensional metamaterial nanotip that has a pyramidal shape. The nanotip itself is made of a large number of densely packed metallic nanospheres. In analogy to the emergence of a continuous energy band in a crystal, the strong coupling among neighboring nanospheres forces them to act collectively and allows the observation of a broad plasmonic band. The largely increased degrees of freedom within the metamaterial nanotip allow to sustain a great variety of different localized eigenmodes. In this contribution, we systematically reveal their peculiar polarization state and show that they allow for light localization in various well-defined spatial domains.

DOI: 10.1103/PhysRevB.81.075317 PACS number(s): 78.20.Ek, 73.20.Mf

I. INTRODUCTION

During the past decades, the desire to localize light and to steer its flow on length scales much less than the wavelength fostered research in the field of plasmonics.[1] There, the essential ingredient is the coupling of the electromagnetic field to the carrier density oscillation in a noble metal leading to the formation of plasmon polaritons. They exhibit properties of both individual excitations in a single eigenmode, where both the beneficial and the detrimental characteristics are allowed to be balanced at will. If the electromagnetic contribution dominates the excitation, it is characterized by a low dissipation, but large mode volumes. By contrast, highly localized fields, but exhibiting large losses, are observed the larger the share of the plasmonic contribution. Plasmon polaritons may be observed as two different specimen. Localized plasmon polaritons are sustained by small metallic nanoparticles whereas propagating plasmon polaritons are confined surface waves at the interface between a metal and a dielectric. The resonantly enhanced interaction between light and matter led to the proposal to use plasmonic elements in a large variety of applications. Examples are nanometric waveguides,[2] biosensing applications,[3] optical data storage,[4] or photon management in solar cells.[5]

After having understood the properties of these elementary excitations, it became obvious that there are many options to be studied to tailor these properties at will in more complex nanostructures. Most notably, the coupling among individual elements and its impact on the quantities of interest were studied. Referential geometries are two coupled nanospheres[6] or the coupling between a nanoparticle and a flat metallic surface.[7] More complicated structures as ring-disk[8] and dolmen geometries,[9] or even stacked split ring resonators[10,11] were at the focus of interest. In most cases the impact of the coupling on the observable quantities may be explained by a plasmon hybridization theory.[12] In analogy to the molecular orbital theory, it interprets the observable spectra in terms of symmetric and antisymmetric eigenstates that can be excited in coupled plasmonic systems; each leading to specific properties.

Whereas the coupling between a few isolated nanoparticles allows to engineer the scattering properties of localized plasmon polaritons, the dispersion characteristic of propagating eigenmodes can be controlled in either infinitely extended chains or three-dimensional periodic arrangements of nanoparticles.[13] The latter artificial material is usually coined an optical metamaterial. Most notably, dispersion characteristics became amenable which are inaccessible by natural occurring materials.[14,15] The topic attracted a great deal of interest since suitably tailored metamaterials allow to implement applications that were unimaginable before where the most prominent example might be the cloaking device.[16]

However, most investigations focus on infinitely extended structures leaving aside those of finite spatial extension with a specific shape and formed by a large number of strongly coupled plasmonic entities. Then, both geometric features, the *inner* and the *outer*, strongly affect either the scattering or the wave guiding properties of the complex structure. A prominent example is a sphere made of densely packed small metallic nanoparticles.[17] The inner geometry causes a material dispersion being reminiscent to an oscillator. The eigenfrequency, the line width, and the oscillator strength of the localized plasmon polariton resonance (leading to an effective permittivity with a Lorentzian shape) are dictated by the properties of the strongly coupled metallic nanoparticles. Forming a sphere out of such tiny spheres allows to observe strong Mie resonances at wavelengths slightly larger than the resonance wavelength. Such materials were recently realized[18] and first approaches to employ self-organization schemes for their fabrication were put forward.[19,20] Other optical elements that can be implemented using densely packed metallic nanospheres are, e.g., interfaces that sustain the excitation of surface waves even for TE polarization.[21]

As a further geometry, the idea of a metamaterial nanotip was put forward recently.[22] The inner geometry of the suggested two-dimensional device was made of densely packed metallic nanocylinders. The outer geometry was chosen to be an equilateral triangle. Depending on various parameters, the structure could be tailored to either strongly localize the light at the surface or inside the nanotip, or to cause the light to

focus behind the nanotip with a large focal depth at a predefined wavelength. For an identical purpose a similar two-dimensional structure was investigated made of closely spaced metal-insulator-metal waveguides.[23]

In this contribution, we extend this idea toward a genuine three-dimensional (3D) metamaterial nanotip with a pyramidal shape. It is made of a large number of strongly coupled metallic nanospheres. By illuminating the nanotip with a linearly polarized plane wave, we reveal the appearance of a band of plasmonic resonances which increases with the spatial extension of the nanotip. The peculiar polarization states and the localization of the electromagnetic field in different spatial domains, namely, in front of, inside, or behind the nanotip, is revealed. We show that eigenmodes excited at shorter wavelengths with respect to the resonance wavelength of the isolated metallic nanosphere are dominated by local field components that deviate from the incident polarization. Eigenmodes at larger wavelengths preserve the polarization. The spatial domain of the largest field enhancement is closer to the base of the nanotip the larger the wavelength is. The behavior is explained in terms of a simple dipole-dipole interaction model. In a complementary explanation, we show furthermore that the spectral domain where such eigenmodes can be excited coincides with that one where the inner geometry has an effective permittivity with a negative real part. Eventually the potential of such nanotips for various applications is discussed.

II. MODEL

To provide a comprehensive understanding, we start our analysis by shortly outlining the numerical methods used to compute all quantities of interest. The computation relies on a rigorous solution of Maxwell's equations where we take explicit advantage of the spherical shape of the inclusions the structure is made of. For this purpose we rely on the framework of Mie theory extended toward the interactions of a large number of spheres with an illuminating field in a self-consistent manner. Details on the algorithm may be found elsewhere.[24,25]

We consider an arrangement of N nonintersecting spheres with radii a^j made of a local, linear, homogenous, and isotropic material with permittivity $\varepsilon^j(\omega)$ and permeability $\mu^j(\omega)$. The superscript $j=1,\ldots,N$ designates the jth sphere of the arrangement. Furthermore we suppose that the surrounding medium is nonabsorbing with material parameters $\varepsilon(\omega)$ and $\mu(\omega)$. From now on, all equations are formulated in Fourier space with electric and magnetic fields $\mathbf{E}(\mathbf{r},\omega)$ and $\mathbf{H}(\mathbf{r},\omega)$ oscillating at an angular frequency ω where for the sake of brevity the arguments are omitted as well as the time dependence $exp(-i\omega t)$.

The ensemble of spheres is illuminated by an external field $\mathbf{E}_{inc}$. In the spherical coordinate system (r,θ,φ) centered at the jth sphere, one can decompose the entire electric field $\mathbf{E}$ into an incident $\mathbf{E}^j_{\mathrm{inc}}$ and a scattered $\mathbf{E}^j_{\mathrm{sca}}$ outside and an internal $\mathbf{E}^j_{\mathrm{int}}$ field inside the jth sphere. Here, the incident field $\mathbf{E}^j_{\mathrm{inc}}$ consists of the external field $\mathbf{E}_{\mathrm{inc}}$ and the scattered fields of all other spheres. Following Mie's theory for a single sphere, these fields are expressed by linear combinations of vector spherical harmonics (VSH) $\mathbf{N}$ and $\mathbf{M}$ which are the analytical eigenmodes of the system (analogous equations are available for the magnetic field)[24]

$$\mathbf{E}^j_{\mathrm{inc}} = -\sum_{l=1}^{\infty}\sum_{m=-l}^{l} iE_{lm}(p^j_{lm}\mathbf{N}_{lm} + q^j_{lm}\mathbf{M}_{lm}), \tag{1}$$

$$\mathbf{E}^j_{\mathrm{int}} = -\sum_{l=1}^{\infty}\sum_{m=-l}^{l} iE_{lm}(d^j_{lm}\mathbf{N}_{lm} + c^j_{lm}\mathbf{M}_{lm}), \tag{2}$$

$$\mathbf{E}^j_{\mathrm{sca}} = \sum_{l=1}^{\infty}\sum_{m=-l}^{l} iE_{lm}(a^j_{lm}\mathbf{N}_{lm} + b^j_{lm}\mathbf{M}_{lm}), \tag{3}$$

where E_{lm} are scaling factors to keep the formulation of multisphere scattering theory consistent with Mie's theory for a single sphere. They are given by

$$E_{lm} = |\mathbf{E_0}|i^l(2l+1)\frac{(l-m)!}{(l+m)!}, \tag{4}$$

with $|\mathbf{E_0}|$ being the magnitude of the external incident field. Applying the boundary conditions at the surfaces of the spheres a correlation between the coefficients of the incident fields p^j_{lm}, q^j_{lm} and the scattered fields a^j_{lm}, b^j_{lm}, as well as for the internal fields c^j_{lm}, d^j_{lm} can be derived

$$a^j_{lm} = a^j_l p^j_{lm}, \quad b^j_{lm} = b^j_l q^j_{lm}, \tag{5}$$

$$c^j_{lm} = c^j_l q^j_{lm}, \quad d^j_{lm} = d^j_l p^j_{lm}. \tag{6}$$

The quantities $a^j_l, b^j_l, c^j_l, d^j_l$ are the Mie coefficients of the isolated jth sphere (see Ref. 26 for explicit equations) which are functions of two normalized terms; the size parameter x^j and the relative refraction coefficient m^j, which are given by

$$x^j = \omega_0\sqrt{\varepsilon\mu}a^j, \quad m^j = \sqrt{\frac{\varepsilon^j\mu^j}{\varepsilon\mu}}. \tag{7}$$

As mentioned before the field $\mathbf{E}^j_{\mathrm{inc}}$ incident on the surface of the jth sphere consists of two parts; the external incident field $\mathbf{E}_{\mathrm{inc}}$ and the scattered fields from all the other spheres transformed into the coordinate system of the jth one

$$\mathbf{E}^j_{\mathrm{inc}} = \mathbf{E}_{\mathrm{inc}} + \sum_{k\neq j}\mathbf{E}_{\mathrm{sca}}(k,j), \tag{8}$$

where (k,j) denotes the transformation from the kth to the jth coordinate system. The global incident field may be expanded in terms of VSH with coefficients p^{j0}_{lm}, q^{j0}_{lm}. An expression for the contribution of the scattered field from the kth sphere to the incident field on the jth sphere is obtained by a translation of the VSH from one spherical coordinate system (r',θ',φ') to another (r,θ,φ). It is given by the translational addition theorem as

$$\mathbf{M}_{lm} = \sum_{l'=1}^{\infty}\sum_{m'=-l'}^{l'}[A0^{lm}_{l'm'}\mathbf{M}'_{l'm'} + B0^{lm}_{l'm'}\mathbf{N}'_{l'm'}], \tag{9}$$

$$\mathbf{N}_{lm} = \sum_{l'=1}^{\infty} \sum_{m'=-l'}^{l'} [B0^{lm}_{l'm'} \mathbf{M}'_{l'm'} + A0^{lm}_{l'm'} \mathbf{N}'_{l'm'}]. \quad (10)$$

The definition of the translation coefficients $A0^{lm}_{l'm'}, B0^{lm}_{l'm'}$ can be found in Refs. 27 and 28. They depend on the distance and orientation between the above introduced two coordinate systems. Inserting Eqs. (9) and (10) into Eq. (8) and accounting for the boundary conditions (5) and (6), we obtain a linear set of equations in terms of the scattering coefficients[25]

$$a^j_{lm} = a^j_l \Bigg\{ p^{j_0}_{lm} - \sum_{k \neq j}^{(1,N)} \sum_{l'=1}^{\infty} \sum_{m'=-l'}^{l'} [a^k_{l'm'} A^{l'm'}_{lm}(k,j) + b^k_{l'm'} B^{l'm'}_{lm}(k,j)] \Bigg\},$$

$$b^j_{lm} = b^j_l \Bigg\{ q^{j_0}_{lm} - \sum_{k \neq j}^{(1,N)} \sum_{l'=1}^{\infty} \sum_{m'=-l'}^{l'} [a^k_{l'm'} B^{l'm'}_{lm}(k,j) + b^k_{l'm'} A^{l'm'}_{lm}(k,j)] \Bigg\}, \quad (11)$$

with a normalized form of the translation coefficients

$$A^{lm}_{l'm'} = \frac{E_{lm}}{E_{l'm'}} A0^{lm}_{l'm'}, \quad B^{lm}_{l'm'} = \frac{E_{lm}}{E_{l'm'}} B0^{lm}_{l'm'}. \quad (12)$$

All scattering coefficients a^j_{lm}, b^j_{lm} can be determined by solving the linear system (11). The coefficients c^j_{lm}, d^j_{lm} for the internal fields result from Eqs. (5) and (6). Thus, the entire fields can be expressed as the sum of the field Eqs. (1)–(3) over all spheres that form the cluster.

Since quasianalytical expressions for the electric and magnetic field in terms of the scattering amplitudes are at hand, formulas for the extinction and scattering cross-sections can be derived that only take into account the coefficients of the scattered a^j_{lm}, b^j_{lm} and the external incident field $p^{j_0}_{lm}, q^{j_0}_{lm}$. Explicit expressions can be found in Ref. 25. With this rigorous framework, all quantities of interest can be computed, namely, the local electromagnetic field and the extinction and scattering cross sections.

III. OPTICAL PROPERTIES OF THE NANOTIP

We now turn out attention to the physical properties of the structure under consideration. The nanotip considered is made of identical silver nanospheres with radii $a^j = 2$ nm illuminated by a plane wave (magnitude $|\mathbf{E_0}| = 1$ V/m) propagating from the base to the apex of the pyramid. It exhibits a linear polarization parallel to one side of the quadratic base (specifically we assume in the following z polarized light propagating in the positive y direction). Material parameters of silver were taken from literature.[29] The surrounding material is a dielectric with a nondispersive permittivity of $\varepsilon(\omega) = 2.25$. Although implementing the structure seems to be challenging, there are promising approaches for their fabrication as self-organization in, e.g., dendritic molecules.[20] In Fig. 1, the structure of the 3D nanotip is shown; silver nanospheres are organized in layers with a distance of Λ to each other; Λ is also the lattice constant of the square lattice where the nanospheres are located in every layer. Succeeding layers are arranged according a close-packing scheme of spheres.

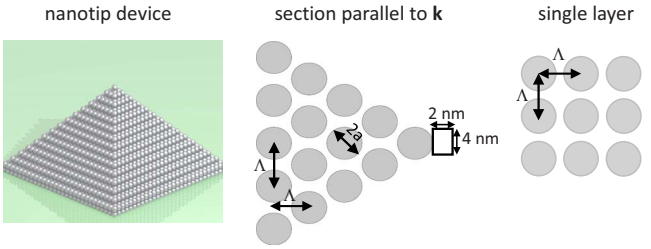

FIG. 1. (Color online) Composition of the 3D nanotip made of periodically arranged, identical nanospheres with diameter $d = 2a$ and period Λ. The small rectangle depicts the interval where the electric field is integrated later on.

Concerning the convergence of our implemented algorithm (that uses the formulation from Sec. II), we considered an angular momentum expansion up to the fourth order; that means the index l runs from one to four in all previous mentioned equations. This threshold is well documented in literature[25] for a given radius of the spheres and a chosen wavelength; also, a crosscheck shows no significant modification using three or four orders. Such a full angular momentum evaluation up to the fourth order causes in a huge computation effort and therefore the calculation of a single point in spectra takes about one day for a pyramid containing 10 layers.

To access the spectral position of plasmonic resonances sustained by the system, we have computed the extinction cross section of such a pyramid as a function of the wavelength at first. Results are shown in Fig. 2. Local maxima depict resonances of the system. Two classes of modes arise. They are characterized by a resonance wavelength shifted to

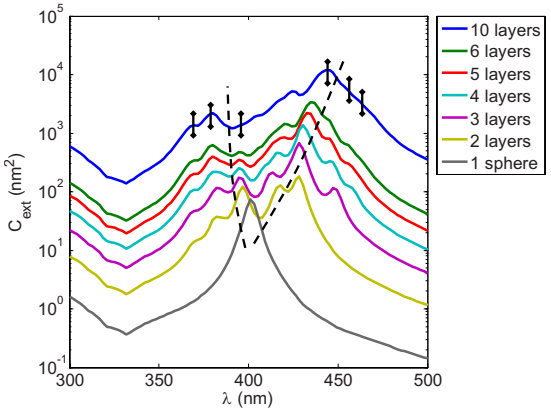

FIG. 2. (Color online) Extinction cross section as a function of the free-space wavelength for several numbers of nanotip layers ($d = 4$ nm, $\Lambda = 4.8$ nm). Vertical bars indicate the wavelengths where field distributions are investigated in detail; see Figs. 3–5 and Fig. 7.

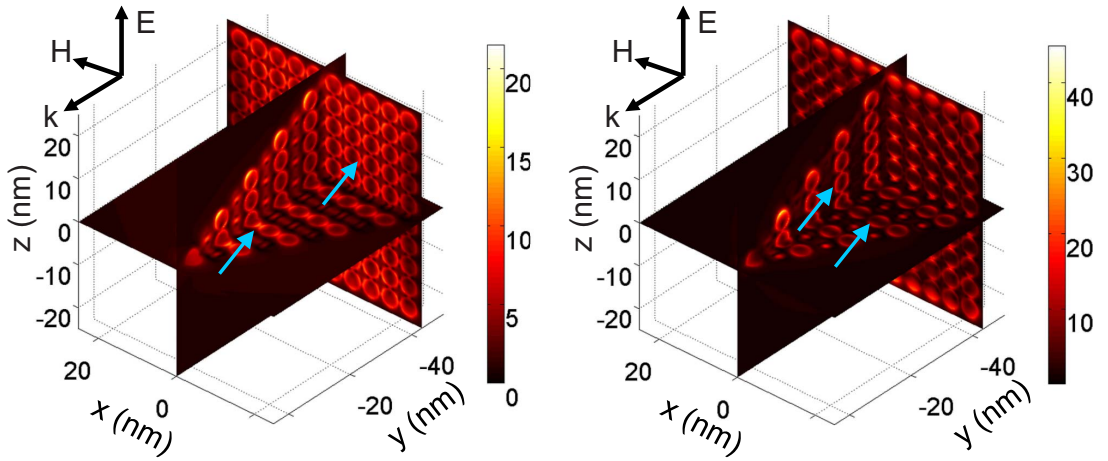

FIG. 3. (Color online) Electric field amplitude in a nanotip (d=4 nm, Λ=4.8 nm) containing 10 layers at the resonance wavelengths λ=370 nm (left panel) and λ=380 nm (right panel). Colored arrows depict essential spatial domains where the mutual coupling of nanospheres can be explained by looking at the field distribution.

either smaller or higher wavelengths compared to the resonance of the single nanosphere (which is defined by an excitation of a localized surface plasmon). This shift increases with the number of nanotip layers. Consequently, a plasmonic band arises as can be seen in Fig. 2. The spectral width converges to a specific value (indicated by the dashed lines in Fig. 2) which is in analogy to solid state physics. There, a crystalline material is formed by assembling a larger number of atoms or molecules, such that their isolated energy states form a band.

An explicit investigation of the field distributions for various resonances will reveal a deeper insight into the optical response of the nanotip and allow us to classify the eigenmodes in well-known theoretical models for coupled nanospheres. In Fig. 3, the amplitude of the electric field (with respect to the incident field) for the resonances excited at 370 and 380 nm for a nanotip containing 10 layers are shown (a selection of special planes offers a quasi-three-dimensional plot). The first resonance is dominated by a mutual coupling of the silver nanospheres parallel to the magnetic field component of the incident field whereas the latter seems to be dominated by a coupling along the propagation direction of the incident plane wave (see colored arrows at the figures). In both cases, the response is dominated by an electric field component not contained in the incidence field. This can be seen from the dipolar character of the field around each nanosphere that is oriented perpendicular to the polarization direction of the incident electric field. The occurrence of the resonance at wavelengths smaller than the resonance wavelength of the isolated nanosphere can be explained by a simple dipole-dipole interaction model.[6] It was established to predict spectral resonance positions for two closely spaced nanospheres. If the interaction occurs parallel to the polarization of the electric field, the resonance is shifted to lower frequencies. The opposite holds for eigenmodes that are dominated by a coupling perpendicular to the polarization. This feature is explained by associating the electric dipoles excited in each nanosphere with a spring characterized by a spring constant that will lead to a resonance frequency. For serially arranged springs, the reciprocal effective spring constant is the sum of the reciprocal individual spring constants, hence the resonance frequency decreases whereas for springs connected in parallel the spring constants add and the resonance frequency increases. This is exactly what we observe.

Therefore, the modes excited at longer wavelengths in Fig. 2 are expected to exhibit a field concentration dominated

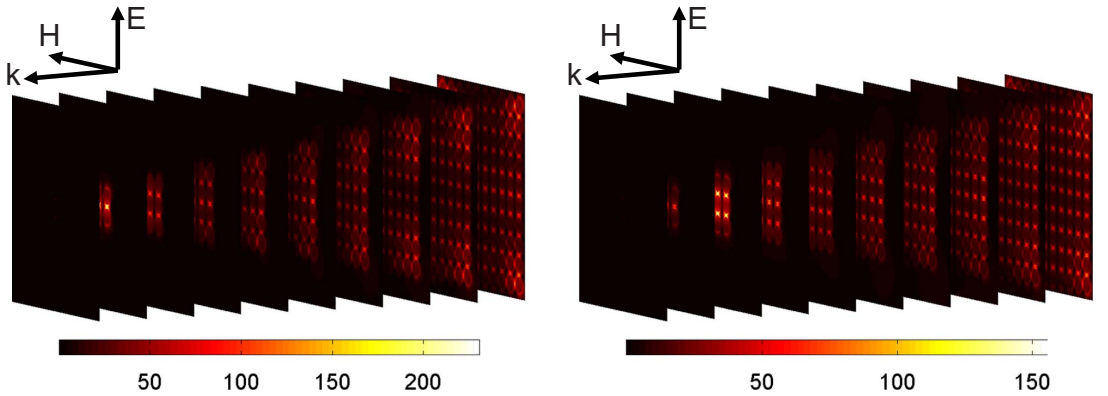

FIG. 4. (Color online) Electric field amplitude in a nanotip (d=4 nm, Λ=4.8 nm) containing 10 layers at the resonance wavelengths λ=445 nm (left panel) and λ=454 nm (right panel).

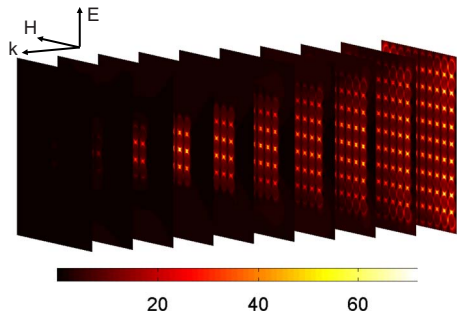

FIG. 5. (Color online) Electric field amplitude in a nanotip (d=4 nm, Λ=4.8 nm) containing 10 layers at the resonance wavelength λ=462 nm.

by the electric field component of the incident field. Exactly this behavior can be observed in Fig. 4. There, the electric field amplitude is shown for eigenmodes that arise at higher wavelengths than the resonance wavelength of the isolated nanosphere. The nanospheres interact along the polarization direction of the illuminating electric field and a remarkable field enhancement of ≈200 with respect to the incident field appears. Also a wavelength-dependent shift in the field maximum can be observed where it is closer to the base for increasing wavelengths; this is confirmed by the field distribution shown in Fig. 5 at λ=462 nm. It can be seen that the largest field enhancement occurs for this wavelength in the forth layer, whereas it was before in the third and in the second layer, respectively (by starting to count at the apex). To elucidate this behavior in detail, it is useful to investigate the magnitude of the scattering dipole coefficients associated with the field component of the incident field across the nanotip. If the incident field is propagating along to the y axis and is polarized along the z direction, the scattering coefficients a_{10}^{j} describe a dipole along the electric field component.

The average magnitude of the coefficients a_{10}^{j} including all nanospheres of a particular plane (1 indicates the apex and "10" the base) as a function of the wavelength is shown in Fig. 6. The behavior previously found has been excellently confirmed, namely, increasing the wavelength leads to a change in the localization of the maximum. It is shifted from the apex to the base with an increasing wavelength. More-

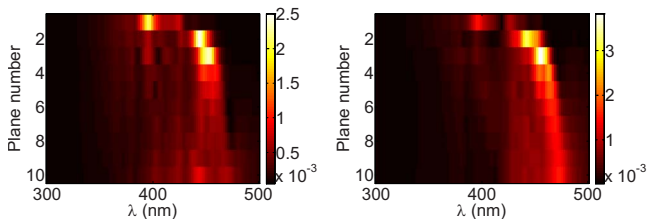

FIG. 6. (Color online) Magnitude of the dipole coefficient a_{10} as a function of the wavelength and the respective plane. The coefficients a_{10}^{j} of every single nanosphere are averaged over all nanospheres in a particular plane (1 indicates the apex and 10 the base of the nanotip) and normalized to the respective coefficient of the incident field. The left and the right panel apply to a pyramid analogous to Fig. 1 (d=4 nm, Λ=4.8 nm) and a pyramid with identical parameters where only the shell contains nanospheres, respectively.

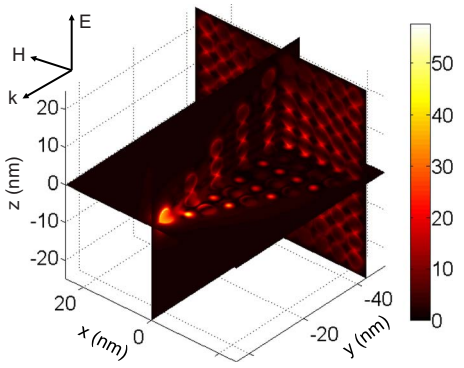

FIG. 7. (Color online) Electric field amplitude in a nanotip (d=4 nm, Λ=4.8 nm) containing 10 layers at the resonance wavelength λ=395 nm.

over, the resonances become wider. In passing, we mention that a similar behavior is observed for a nanotip consisting only of the outer shell of nanospheres. The results displayed in the right panel of Fig. 6 clearly indicates that the excited eigenmodes are dominated by the coupling of adjacent nanospheres and not by the pyramidal geometry. Hence, alternative outer geometries should exhibit the same resonances and only the inner geometry controls their very spectral position.

The ability to control the position of maximum field enhancement by adjusting the illumination wavelength, allows to operate the nanotip in a regime where it occurs near the apex. The respective wavelength is λ=395 nm, as can be seen in Fig. 6 (the resonance can be also traced in Fig. 2) and the associated electric field amplitude is shown in Fig. 7. However, due to geometrical peculiarities the field enhancement directly at the apex is not as large as the field enhancement inside the bulk of the nanotip. At the apex, no coupling occurs along the polarization direction of the electric field since only a single nanosphere forms the apex and only a weak coupling to nanospheres in the second plane is encountered. In the dipole-dipole interaction model previously mentioned, the consequence is a small shift to shorter wavelengths with respect to the single nanosphere resonance. Also, the field enhancement turned out much smaller than

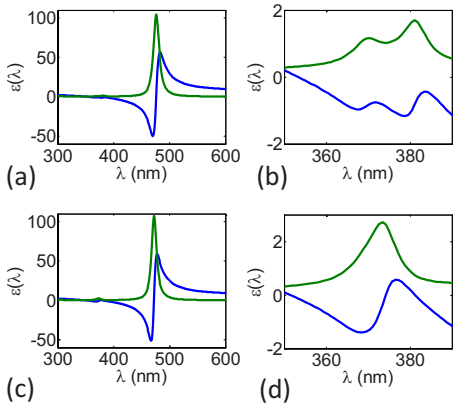

FIG. 8. (Color online) Effective permittivities (blue graph: real part, green graph: imaginary part) as a function of the wavelength for two different MMs (see text). (a), (b): closely packed spheres as mentioned in Fig. 1; (c), (d): spheres on a square lattice.

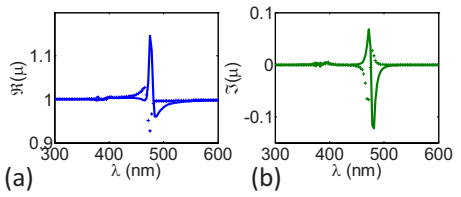

FIG. 9. (Color online) Effective permeabilities [(a): real part, (b): imaginary part] as a function of the wavelength for two different MMs (see text). The dashed graph depict a structure as mentioned in Fig. 1 and the solid graph is related to a square lattice.

that of the other modes, which are dominated by the dipole coefficients a_{10}. As a consequence, a substantial field concentration is only feasible if a mutual coupling of nanospheres along the polarization direction of the incident electric field exists. Truncating the apex of the nanotip might lift the problem, though it is not a favorable solution.

To finally identify the exact spectral domain where eigenmodes can be excited, we have analyzed the effective properties of metamaterials (MM) made of the densely packed nanospheres. We distinguish two geometries. The first MM comprises nanospheres arranged on a square lattice at a singular plane. The second MM consists of unit cells made of two layers of the same lattice but mutually shifted by half a period in lateral direction to form the closely packed sphere geometry as considered for the nanotip. Results for the effective permittivity of both geometries are shown in Fig. 8. Effective properties were rigorously obtained from transmission/reflection data of a MM slab.[30] We ensured that the effective properties converged for an increasing number of functional layers forming the slab. To obtain the transmission and reflection coefficients of periodically arranged nanospheres, an appropriate algorithm was used to compute these quantities.[31] Both MM dispersion curves associated with the permittivity exhibit a Lorentzian resonance located at ≈470 nm. This wavelength corresponds to the largest wavelength where the inner geometry effectively acts like a metal. For even larger wavelengths, the effective permittivity is positive and the inner geometry rather acts as a dielectric. This wavelength is in excellent agreement with the upper bound of eigenmodes that can be excited in the nanotip; as seen in Fig. 6. The wavelength of the Lorentzian resonance of the effective permittivity $\varepsilon_{\text{eff}}(\omega)$ coincides with the wavelength of the eigenmode, which exhibits a field concentration at the base of the pyramid. Therefore, the shift in the field maximum toward the base with increasing illumination wavelength is nicely explained by the underlying material dispersion. Since slightly below resonance the real part of the permittivity attains large negative values and the imaginary part becomes large, the inner geometry acts like a perfect metal in this spectral domain. Thus, light is rejected from the nanotip and the effective skin depth is very small. Therefore, we observe a shift in the field maximum toward the base for wavelengths approaching the resonance of $\varepsilon_{\text{eff}}(\omega)$. At smaller wavelengths, the penetration depth is larger and the spatial position of the largest field concentration occurs in the bulk of the nanotip.

The MM with closely packed nanospheres exhibits two additional resonances, related to eigenmodes, at 370 and 380 nm [see Fig. 8(b)] clearly to be recognized by the local maxima of the imaginary part of $\varepsilon_{\text{eff}}(\omega)$. For the square lattice geometry, the resonance at 380 nm disappears. Therefore, we conclude that the resonance at 370 nm is induced due to a strong intraplane coupling among neighboring nanospheres. This resonance is associated with the field distribution shown in Fig. 3 (left panel). By contrast, the other mode at 380 nm occurs due to a strong inter-plane coupling among neighboring nanospheres in adjacent planes. This is in perfect agreement with the field distribution as shown in Fig. 3 (right panel), where it was noticed that a longitudinally polarized field dominates the internal field of the nanotip. Contrary to observations for two-dimensional nanotips,[22] no modes were observed associated with a dielectric behavior in the effective material at wavelengths larger than 470 nm. This is most likely a consequence of the small spatial perimeter of the nanotip with respect to the wavelength. An increase in the spatial extension of the nanotip is presently not possible due to the restricted computational resources. For completeness, we also show in Figs. 9(a) and 9(b) the effective permeability as retrieved for the present structure. Although a minor dispersion can be observed, we are confident that it is too weak to allow for possible further applications in the context of the nanotip as discussed in literature.[32]

As a first summary, the major resonance of the effective permittivity at 470 nm arises due to the mutual coupling of adjacent nanospheres along the polarization direction of the electric field. The huge negative real part of $\varepsilon_{\text{eff}}(\omega)$ at slightly shorter wavelengths leads to a remarkable field concentration into particular planes of the nanotip. A smaller real part of the effective permittivity permits for a larger penetration of the electromagnetic field at a minor damping. The mode at 395 nm (where the maximum field enhancement is generated at the apex) can be understood as result of a optimal ratio between wavelength and extension of the pyramid. Thus, at that wavelength, one may take advantage of the properties of this mode and the nanotip may be used for applications that require a strong field enhancement in narrow spatial domains. To quantitatively estimate this enhancement, an integration of the electromagnetic field in a 3D interval (as sketched in Fig. 1) was performed. It turned out that the field enhancement at the apex of a nanotip exceeded that of a single nanosphere by 10%. Furthermore, there is a remarkable field enhancements (≈200 times larger than the incident field) inside the nanotip. This may provide a route to use such structures too as porous materials in, e.g., surface-enhanced Raman scattering (SERS) applications. Because of the nonlinear response of the SERS signal, the field enhancement at the apex might be useful, although when compared to a single nanosphere the results are not very impressive. The shell pyramid does not exhibit an appreciable field concentration at the apex but the localization in the other planes compares to that in the previous example. This is obvious by comparing the dipole coefficients in Fig. 6.

IV. DISCUSSION AND CONCLUSIONS

We examined a three-dimensional nanotip made of small silver nanospheres embedded in a dielectric host medium. An

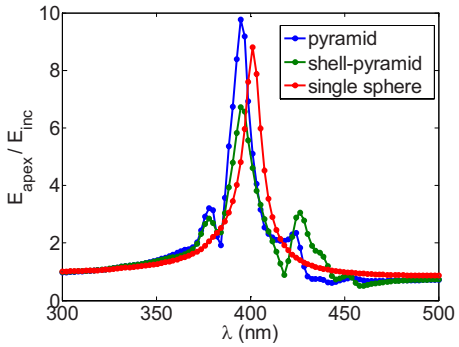

FIG. 10. (Color online) Integrated electric field as a function of the wavelength in a three-dimensional interval at the apex of the nanotip (see Fig. 1). All graphs are normalized to the incident field in the interval.

illumination with a plane wave excited various eigenmodes that allowed to concentrate the electric field into particular spatial domains. The entire behavior of the nanotip was qualitatively described by well-known theoretical models as the dipole-dipole interaction[6] and the effective medium model. We showed that the Lorentzian dispersion of the effective permittivity arose from the mutual coupling of adjacent nanospheres in the same layer and only one mode is affected by the complete geometry of the pyramid.

From Fig. 10, one could conclude that nanotips of plasmonic nanospheres are not prospective for sensing and microscopic applications. Indeed, the maximum possible local field enhancement at the apex compares to that of an isolated nanosphere illuminated with a plane wave. However, this result should be considered as preliminary and further detailed considerations revealed encouraging aspects.

A prospective application of such a nanotip could be its use as a probe in a scanning near-field optical microscope (SNOM) enabling a resolution down to 10 nm and compare the present structure against competing tips. A dielectric nanotip for an aperture-type is not suitable for this purpose. It would create a smaller field enhancement at a worse resolution. A nanotip consisting of bulk metal and used in atomic force microscope and apertureless SNOM will create the same field enhancement near the apex. However, the major part of the field energy will be scattered by the metal tip and not by a nano-object to be probed. In this approach, it is a serious issue to discriminate the response of the tip from that of the object to be probed. This problem is solvable in our approach, in principle, by introducing an adiabatic change in the permittivity profile by inducing a gradient in the spatial separation among neighboring spheres from the base to the apex. This would permit to adiabatically squeeze the light into the region of interest.

A dielectric nanotip covered with metal and comprising an aperture of diameter less than 10 nm is an evident competitor for the structure under study in terms of achievable spatial resolution. However; its intrinsic disadvantage is its low power throughput. In terms of efficiency, it can compete with the metamaterial nanotip only if the effect of extraordinary transmission would be exploited. To observe such extraordinary transmission requires the use of a nanocorrugated metal film covering the tip.[33] Such assisting structures are not easy to manufacture, and the structure under considerations stays competitive and the promise of a higher throughput should be sufficient motivation for an extra effort.

With the perspective application of a SNOM tip in mind, one may hypothesize to use a dielectric tip equipped with a plasmonic nanoparticle at the apex. In accordance with Fig. 10 at first glance such structure creates the same local field as our metamaterial nanotip. However, a closer look reveals that this is not true. The hot spot created by the dielectric tip itself will partially mask the spot created by the nanoparticle, hence, drastically decreasing the possible spatial resolution. Also, the scattering will be probably higher in this case. The potential of the metamaterial nanotip is higher than the potential of the dielectric nanotip with a metal particle at the termination. As it was explained in Ref. 22, the metamaterial nanotip connected to a core of a dielectric waveguide potentially allows to suppress both scattering and reflection of the incident beam. The reflection can be suppressed by matching the effective permittivity of the metamaterial to that of the dielectric waveguide. The present numerical study (Figs. 3–7) shows that scattering through the lateral walls of the nanotip practically disappears as it was predicted for 3D metamaterial nanotips in Ref. 22. As a result, the entire energy of the incident light beam can be transmitted into the nanotip and concentrated in its bulk as well as at the hot spot near the apex. The scattered light outside the nanotip will be fully determined by the nano-object (if there is one inside the hot spot). Having these speculations in mind, we consider metamaterial nanotips as a prospective tool for sensing and probing applications.

ACKNOWLEDGMENTS

Financial support by the Federal Ministry of Education and Research (PHONA), from the State of Thuringia within the ProExcellence program (MEMA), as well as from the European Union (NANOGOLD) is acknowledged.

[1] S. A. Maier, *Plasmonics: Fundamentals and Applications*, 1st ed. (Springer, Berlin, 2007).
[2] E. Feigenbaum and M. Orenstein, Opt. Express **14**, 8779 (2006).
[3] D. Cialla, R. Siebert, U. Huebner, R. Moeller, H. Schneidewind, R. Mattheis, J. Petschulat, A. Tuennermann, T. Pertsch, B. Dietzek, and J. Popp, Anal. Bioanal. Chem. **394**, 1811 (2009).
[4] T. Arai, K. Kurihara, T. Nakano, J. Tominaga, and C. Rockstuhl, Appl. Phys. Lett. **88**, 051104 (2006).
[5] A. Luque, A. Marti, M. J. Mendes, and I. Tobias, J. Appl. Phys. **104**, 113118 (2008).
[6] W. Rechberger, A. Hohenau, A. Leitner, J. R. Krenn, B. Lamprecht, and F. R. Aussenegg, Opt. Commun. **220**, 137 (2003).
[7] A. Christ, T. Zentgraf, S. G. Tikhodeev, N. A. Gippius, O. J. F. Martin, J. Kuhl, and H. Giessen, Phys. Status Solidi B **243**, 2344 (2006).
[8] N. Verellen, Y. Sonnefraud, H. Sobhani, F. Hao, V. V. Mosh-

chalkov, P. Van Dorpe, P. Nordlander, and S. A. Maier, Nano Lett. **9**, 1663 (2009).
[9] F. Hao, P. Nordlander, Y. Sonnefraud, P. Van Dorpe, and S. A. Maier, ACS Nano **3**, 643 (2009).
[10] N. Liu, L. Fu, S. Kaiser, H. Schweizer, and H. Giessen, Adv. Mater. **20**, 3859 (2008).
[11] N. Liu, H. Liu, S. Zhu, and H. Giessen, Nat. Photonics **3**, 157 (2009).
[12] E. Prodan, C. Radloff, N. J. Halas, and P. Nordlander, Science **302**, 419 (2003).
[13] C. Rockstuhl, C. Menzel, T. Paul, T. Pertsch, and F. Lederer, Phys. Rev. B **78**, 155102 (2008).
[14] M. G. Silveirinha, C. A. Fernandes, J. R. Costa, and C. R. Medeiros, Appl. Phys. Lett. **93**, 174103 (2008).
[15] C. R. Simovski and S. A. Tretyakov, Phys. Rev. B **79**, 045111 (2009).
[16] U. Leonhardt, Science **312**, 1777 (2006).
[17] C. Rockstuhl, F. Lederer, C. Etrich, T. Pertsch, and T. Scharf, Phys. Rev. Lett. **99**, 017401 (2007).
[18] J. H. Lee, Q. Wu, and W. Park, Opt. Lett. **34**, 443 (2009).
[19] X. Zeng, F. Liu, A. G. Fowler, G. Ungar, L. Cseh, G. H. Mehl, and J. E. Macdonald, Adv. Mater. **21**, 1746 (2009).
[20] S. Frein, J. Boudon, M. Vonlanthen, T. Scharf, J. Barberá, G. Süss-Fink, T. Bürgi, and R. Deschenaux, Helv. Chim. Acta **91**, 2321 (2008).
[21] R. Sainidou and F. J. García de Abajo, Opt. Express **16**, 4499 (2008).
[22] C. Rockstuhl, C. R. Simovski, S. A. Tretyakov, and F. Lederer, Appl. Phys. Lett. **94**, 113110 (2009).
[23] W. M. Saj, Opt. Express **17**, 13615 (2009).
[24] D. W. Mackowski, Proc. R. Soc. London, Ser. A **433**, 599 (1991).
[25] Y.-l. Xu, Appl. Opt. **34**, 4573 (1995).
[26] C. F. Bohren and D. R. Huffman, *Absoption and Scattering of Light by Small Particles*, 1st ed. (Wiley, New York, 1983).
[27] A. Stein, Q. Appl. Math. **19**, 15 (1961).
[28] O. R. Cruzan, Q. Appl. Math. **20**, 33 (1962).
[29] P. B. Johnson and R. W. Christy, Phys. Rev. B **6**, 4370 (1972).
[30] C. Menzel, C. Rockstuhl, T. Paul, F. Lederer, and T. Pertsch, Phys. Rev. B **77**, 195328 (2008).
[31] N. Stefanou, V. Yannopapas, and A. Modinos, Comput. Phys. Commun. **132**, 189 (2000).
[32] X. Hu, C. T. Chan, J. Zi, M. Li, and K.-M. Ho, Phys. Rev. Lett. **96**, 223901 (2006).
[33] T. J. Antosiewicz and T. Szoplik, Opt. Express **15**, 10920 (2007).